Journal of Food Engineering 208 (2017) 77–88

Contents lists available at ScienceDirect

Journal of Food Engineering

journal homepage: www.elsevier.com/locate/jfoodeng

The SAOS, MAOS and LAOS behavior of a concentrated suspension of tomato paste and its prediction using the Bird-Carreau (SAOS) and Giesekus models (MAOS-LAOS)

Ozlem Caglar Duvarci [a, b], Gamze Yazar [b], Jozef L. Kokini [b, *]

[a] Chemical Engineering Department, Izmir Institute of Technology, Gulbace Koyu, Urla, Izmir, Turkey
[b] Department of Food Science, Purdue University, West Lafayette, IN 47907, USA

ARTICLE INFO

Article history:
Received 18 October 2016
Received in revised form
14 January 2017
Accepted 27 February 2017
Available online 18 March 2017

Keywords:
SAOS/MAOS/LAOS of tomato paste
Lissajous-Bowditch curve
Strain hardening
Shear thinning

ABSTRACT

The SAOS and LAOS behavior of tomato paste were investigated in this study. SAOS rheology was well predicted by the semi-empirical Bird-Carreau constitutive model. The LAOS (Large amplitude oscillatory shear) behavior of tomato paste was also investigated in depth in this study and non-linear rheological properties were obtained by utilizing Ewoldt-McKinley theory. These parameters offer new insights into the rheology of tomato paste and help understand structural changes which occur at different deformations (strain) and time scales (frequency). We plotted the intracycle normalized stress vs. normalized strain in the linear and non-linear regions offered new intracycle insights and observations. Tomato paste showed an irreversible structural change in LAOS evidenced by strain softening (in the mid-oscillatory region) followed by strain hardening (in the large oscillatory region). The nonlinear flow behavior simulated by the single mode Giesekus model gave good results up to moderate strains and frequencies. These results help gain better insights at large deformations, which occur during processing and consumption.

1. Introduction

Food suspensions like tomato paste are complex multiphase unstable biomaterials and their flow behavior depends on the content and the constituents as well as their concentrations. In spite of considerable work done on characterization of rheological behavior of food materials in steady shear and small oscillatory flow [Bayod et al., 2007; Bayod et al., 2008; Bayod and Tornberg, 2011; Vercet et al., 2002; Valencia et al., 2003; Sahin and Ozdemir, 2004; Chou and Kokini, 1987; Sanchez et al., 2002; Xu et al., 1986; Koocheki et al., 2009; Tanglertpaibul and Rao, 1987; Rao, 2007], their large deformation behavior has not been studied carefully. Understanding the flow behavior of tomato paste in large deformations may give new and more accurate information on both rheological behavior and also structural changes during deformation. This might be useful to improve and optimize flow behavior and processing conditions like thermal processing which would have a reflection on the quality, safety and shelf-life of food products such as tomato paste.

Tomato concentrates exhibit non-Newtonian behavior including yield stresses, shear thinning and shear history dependence which is closely related with concentration (Rao, 2007; Bayod and Tornberg, 2011). The steady shear flow of tomato products mainly showed Bingham plastic flow behavior at low shear rates and Herschel-Bulkley at higher shear rates (Dervisoglu and Kokini, 1986; Agusto et al., 2012) or power law/Casson for less concentrated products (Bayod et al., 2008; Koocheki et al., 2009). It was also reported that tomato suspensions at high concentrations of tomato particles may exhibit rheopectic behavior, especially after homogenization [Bayod et al., 2007]. The pectin in the tomato causes entanglement of particles, which is responsible for the variation of viscosity of tomato products [Bayod and Tornberg, 2011].

The steady shear and oscillatory shear rheology of food dispersions like tomato paste and ketchup are a function of solids content and the morphology, particle size and size distribution of the dispersed phase. Small amplitude oscillatory shear flow properties of many food materials were investigated widely (Bistany and Kokini, 1983a, b; Plutchok and Kokini, 1986; Mills and Kokini,

* Corresponding author.
E-mail address: jkokini@purdue.edu (J.L. Kokini).

http://dx.doi.org/10.1016/j.jfoodeng.2017.02.027
0260-8774/

1984; Wang and Kokini, 1995; Valencia et al., 2003; Sanchez et al., 2002, 2003; Chou and Kokini, 1987; Sahin and Ozdemir, 2004) and gave valuable and insightful information related with the organization and stability of their structure.

Small amplitude oscillatory shear flow has been investigated by observing the strain and frequency dependence of materials and provides information without disturbing the 3D structure of materials significantly. However, in most processing operations, food materials may undergo sudden and large deformations that may change their structure reversibly or irreversibly. Therefore, their behavior in large amplitude oscillatory flow (LAOS) gives additional insights to understand structural changes in large deformations and reveal previously unobserved interesting new structural information that may be useful to offer hints about what to expect during processing and consumption. (Wang and Kokini, 1995; Dogan and Kokini, 2007).

With the recent remarkable work of Ewoldt et al. (2008) where the time dependence in the non-linear region was transformed to a frequency dependence using Fourier transforms and where the strain dependence has been successfully de-convoluted using Chebyshev polynomials, new tools exist to probe the rheology of food materials like tomato paste in much more depth than previously possible.

Recently, there are several publications about nonlinear behavior of structured food materials, such as dough, xanthan gum, egg foams, mashed potato, chocolate, polysaccharides, which showed a rich nonlinear behavior captured with LAOS analysis (Yazar et al., 2016, 2017; van der Vaart et al., 2013; Joyner and Meldrum, 2016; Foungfuchat et al., 2012; Carmona et al., 2014; Ptaszek, 2015; Duvarci et al., 2017; Melito et al., 2013a, 2013b; Szopinski and Gerrit, 2016; Gunasekaran and Ak, 2002; Ng et al., 2011). The structural changes of these different foodstuffs (concentrate suspensions, emulsions, foams, polysaccharide solutions, cheese etc.) were reported and the effect of preparation methods, the constituents and the effects of their concentration/function/performance on nonlinear rheological behavior were investigated.

The objective of this research is to carefully and thoroughly study the LAOS behavior of tomato paste and simulate small amplitude oscillatory (SAOS) and large amplitude oscillatory (LAOS) behavior using constitutive models. We studied tomato paste behavior as a function of frequency and strain, plotted the raw and normalized intracycle stress strain behavior and look at their evolution as a function of both strain and frequency and calculated eight LAOS parameters (G'_L, G'_M, η'_L, η'_M, e_3/e_1 v_3/v_1, S and T), and observed previously unreported strain thickening and strain hardening behavior as a function of the applied strain and frequency. The ability to better understand non-linear rheology and simulate it with non-linear constitutive models offers opportunities to simulate flow processes better as we have done before for extrusion and mixing (Dhanasekharan et al., 2001; Connelly and Kokini, 2003; Vyakaranam and Kokini, 2010; Rathod and Kokini, 2014). Understanding flow processes better always enables the improvement in the design of flow processes for mixing, pipe flow, evaporation and continuous thermal processing.

1.1. Rheological behavior of structured materials in SAOS and LAOS

In the linear viscoelastic region, the fluid's response to a small sinusoidal shear deformation (SAOS) is a proportional sinusoidal stress. If the oscillation creates deformations large enough to be in non-linear region, a deviation in stress response from perfect sine wave shape has been started to observe. Fourier transformation expresses the deformed stress response wave as sum of sine and cosine waves functions and translates from the time domain to the frequency domain [Wilhelm et al., 1998; Kallus et al., 2001; Wilhelm, 2002]. The appearance of higher harmonics occurs at larger amplitudes of strain. The odd symmetry with respect to directionality of shear strain/rate dictates that rheological response is only dependent on odd harmonics and even harmonics may be indicators of measurement errors such as wall slip, secondary flows, and fluid inertia [Cho et al., 2005, Ewoldt et al., 2008, Hyun et al., 2011, Graham, 1995, Reimers and Dealy, 1998, Atalik and Keunings, 2002, Yosick et al., 1998, Dervisoglu and Kokini, 1990].

The plots of the elastic (σ') and viscous (σ'') components are plotted with respect to strain ($\gamma(\%)$) and strain rate ($\dot{\gamma}$), are known as Lissajous-Bowditch (LB) loops leading to sound and rigorous rheological properties. The very narrow elliptical shaped LB curves in elastic perspective (σ' vs γ) and circular LB loops in viscous perspective (σ'' vs $\dot{\gamma}$) indicated solid like material. The LB loops becomes distorted in nonlinear region and the progressive change can be observed by plotting the LB loops at different strains. The elastic and viscous LB loops are circular and very narrow elliptical shaped for a Newtonian like fluid.

The proposed new non-linear rheological properties have been used to interpret physical and structural changes in the non-linear region. The new parameters (LAOS parameters: G'_M, G'_L, η'_L, η'_M, e_3/e_1, v_3/v_1, S and T) defined by Ewoldt et al. (2008) lead to new and previously untapped information on the deformation behavior of complex structured materials. The third-order Chebyshev coefficients (e_3 and v_3) was proposed to be used to interpret the deviations from linearity and to evaluate the local nonlinear viscoelastic behavior of the material. The material's nonlinear behavior is classified in six categories depending the sign of the third Chebyshev polynomials as: strain stiffening when $e_3 > 0$, linear elastic when $e_3 = 0$, strain softening when $e_3 < 0$, shear thickening $v_3 > 0$, linear viscous when $v_3 = 0$, shear thinning when $v_3 < 0$. Other details of these calculations and their interpretation are given in Yazar et al., 2016.

1.2. The Bird-Carreau model for SAOS

The Bird-Carreau model was previously used to simulate wheat flour dough SAOS rheology (Dus and Kokini, 1990). For this model to be tested it is necessary to determine the values of zero-shear viscosity (η), the time constants (λ_1, λ_2, α_1, and α_2) from experimental data.

At low shear rates;

$$\eta = \frac{\eta_p}{1 + (\lambda_{1,p}\dot{\gamma})^2}$$

At high shear rates;

$$\eta = \frac{\pi\eta_p}{Z(\alpha_1) - 1}\cdot\frac{(2^{\alpha_1}\lambda_1\dot{\gamma})^{(1-\alpha_1)/\alpha_1}}{2\alpha_1 \sin\left(\frac{1-\alpha_1}{\alpha_1}\pi\right)}$$

where,

$$\lambda_{1,p} = \lambda_1\left(\frac{1+n_1}{p+n_1}\right)^{\alpha_1},$$

$$\eta_p = \eta_o\left(\frac{\lambda_{1p}}{\sum_{n=0}^{\infty}\lambda_{1p}}\right)$$

$Z(\alpha_1) =$ Reimann's zeta potential.

The first normal stress coefficient is given as,

At low shear rates;

$$\psi_1 = 2\sum_{p=1}^{\infty} \frac{\eta_p \lambda_{1,p}}{1 + (\lambda_{1,p}\dot{\gamma})^2}$$

At high shear rates;

$$\psi_1 = \frac{2^{\alpha_2+1}\lambda_2 \pi \eta_o}{Z(\alpha_1) - 1} \cdot \frac{(2^{\alpha_1}\lambda_1\dot{\gamma})^{(1-\alpha_1-\alpha_2)/\alpha_1}}{2\alpha_1 \sin\left(\frac{1+\alpha_1-\alpha_2}{\alpha_1}\pi\right)}$$

The dynamic viscosity at low and high frequencies can be approximated by using the following equations,

At low frequencies;

$$\eta' = \sum_{p=1}^{\infty} \frac{\eta_p}{1 + (\lambda_{2,p}\omega)^2}$$

At high frequencies;

$$\eta' = \frac{\pi \eta_o}{Z(\alpha_1) - 1} \cdot \frac{(2^{\alpha_2}\lambda_2\dot{\gamma})^{(1-\alpha_1)/\alpha_2}}{2\alpha_2 \sin\left(\frac{1+2\alpha_2-\alpha_1}{2\alpha_2}\pi\right)}$$

The out-of-phase of complex viscosity divided by frequency is given by,

At low frequencies;

$$\eta''/\omega = \sum_{p=1}^{\infty} \frac{\eta_p \lambda_{2,p}}{1 + (\lambda_{2,p}\omega)^2}$$

At high frequencies;

$$\eta''/\omega = \frac{2^{\alpha_2}\lambda_2 \pi \eta_o}{Z(\alpha_1) - 1} \cdot \frac{(2^{\alpha_2}\lambda_2\omega)^{(1-\alpha_1-\alpha_2)/\alpha_1}}{2\alpha_1 \sin\left(\frac{1+\alpha_2-\alpha_1}{2\alpha_2}\pi\right)}$$

1.3. The Giesekus model for prediction of nonlinear (LAOS) behavior of tomato paste

The single-mode Giesekus model was used to describe the nonlinear rheological properties of wheat flour doughs (Dhanasekharan et al., 1999, 2001). The concept of configuration-dependent molecular mobility (α) describes the relationship between the relative motion and generating force. The single-mode Giesekus model can also predict ψ_1 and ψ_2 overshoots in shear and 1st normal stresses in start-up experiment and contains upper convected Maxwell and Jeffrey's models as special cases [Giesekus, 1982; Dhanasekharan et al., 2001; Dogan and Kokini, 2007; Morrison, 2001]. In multi-mode Giesekus model, even though multi-mode Giesekus model is expected to predict the experimental results better, the second relaxation time term in the equations had very little contribution on the stress response calculation, hence single mode of the model was used. Single mode Giesekus model contains four parameters: a relaxation time (λ), the solvent and polymer contributions to zero shear viscosity $\left(\eta_o = \eta_p + \eta_s\right)$ and the dimensionless molecular mobility factor (α) which is associated with anisotropic Brownian motion and anisotropic hydrodynamic drag force acting on the suspended particles.

The differential equations derived from matrix solution is given below:

$$\tau_{xx} + \lambda\frac{\partial}{\partial t}\tau_{xx} - 2\lambda\dot{\gamma}_{xy}\tau_{xy} - \alpha\frac{\lambda}{\eta_o}\left(\tau_{xx}^2 + \tau_{xy}^2\right) = 0$$

$$\tau_{xy} + \lambda\frac{\partial}{\partial t}\tau_{xy} - \lambda\dot{\gamma}_{xy}\tau_{yy} - \alpha\frac{\lambda}{\eta_o}\tau_{yx}(\tau_{xx} + \tau_{yy}) = -\eta_o\dot{\gamma}_{xy}$$

$$\tau_{yy} + \lambda\frac{\partial}{\partial t}\tau_{yy} - \alpha\frac{\lambda}{\eta_o}\left(\tau_{yy}^2 + \tau_{xy}^2\right) = 0$$

$$\tau_{zz} + \lambda\frac{\partial}{\partial t}\tau_{zz} - \alpha\frac{\lambda}{\eta_o}\left(\tau_{zz}^2\right) = 0$$

The study reported in this paper aimed to show the SAOS and LAOS behavior of a concentrated suspension of tomato paste which contains soft particles dispersed in a soluble pectin serum (Chou and Kokini, 1987; Kokini and Chou, 1993) in order to explore the structural evolution experienced in small and large deformations by tomato paste. We studied the linear viscoelastic behavior and simulated the steady shear viscosity, the primary normal stress coefficient as well as the complex viscosity η^* using the Bird-Carreau model followed by understanding the intracycle changes during LAOS and modeling the LAOS behavior using the single-mode Giesekus model.

2. Materials and methods

2.1. Materials

Tomato paste (Hunt) was used as it was purchased from a local supermarket. Once the can was opened it was sealed using paraffin

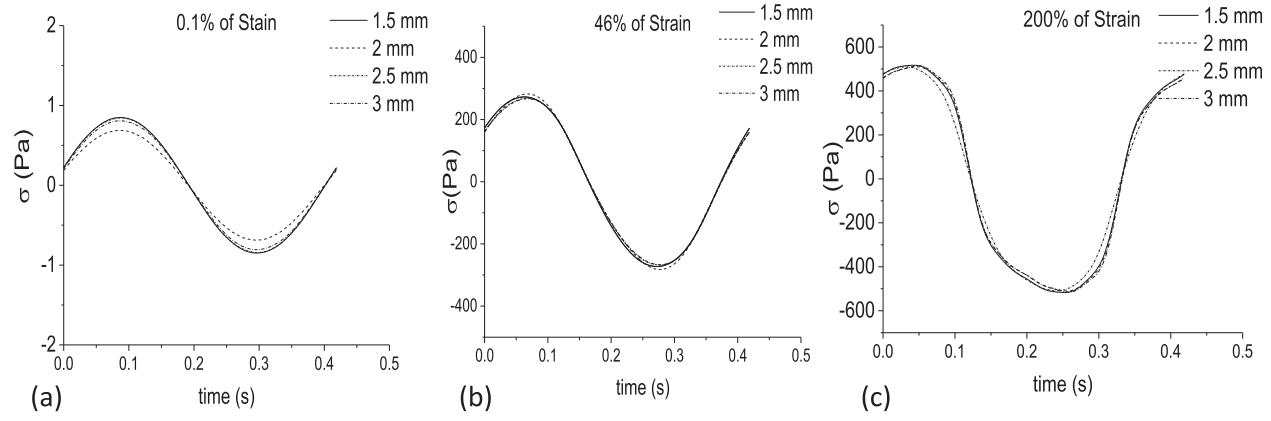

Fig. 1. The reconstructed sine waves after Fourier Transformation of raw data at (a) 2, (b) 10 and (c) 200% of strain with different gap width (1.5, 2, 2.5 and 3 mm).

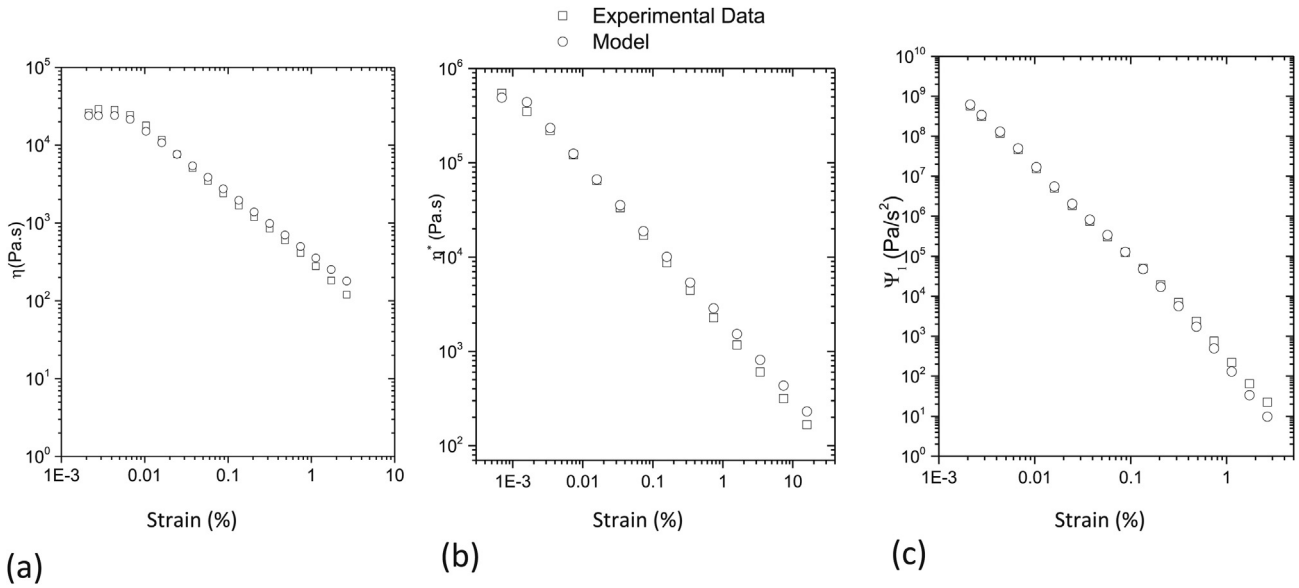

Fig. 2. The comparison of experimental data and the predicted data for (a) η vs $\dot{\gamma}$, (b) ψ_1 vs $\dot{\gamma}$, and (c) η^* vs ω.

paper and aluminum foil to minimize moisture losses and consumed in two days.

2.2. Rheological measurements

The rheological experiments were performed on a stress controlled Discovery Hybrid Rheometer DHR3 from TA Instruments. The strain input produced by using a stress-controlled rheometer is identical with the strain input produced from a strain-controlled rheometer [Bae et al., 2013].

A fresh sample (~2–3 ml) was used for each measurement on a hatched surface parallel plate (40 mm in diameter) geometry with 2 mm gap. The sample was trimmed at the rim of the parallel plate geometry (2.2 mm of gap) with a razor blade and the rim was covered by vegetable oil to eliminate drying during measurement. The sample was allowed to relax until the normal force was lower than 1 N prior to each measurement.

The linear and nonlinear rheology of tomato paste was studied in the strain range of 0.01–210% at different frequencies (0.5, 1, 5, 10, 15 rad/s) with 5 cycles per point. The frequency sweeps were done in a range of 0.1 and 100 rad/s and flow behavior was determined by increasing shear rate from 0.05 to 5 s^{-1}.

The presence of slip during measurements was investigated by conducting strain sweep tests at different gap sizes (1.5, 2, 2.5 and 3 mm) at 15 rad/s. at 0.01, 46 and 200% strain. The stress waves after Fourier transformation using TA instruments' Trios Software (v.2.6) were plotted with respect to time in Fig. 1 as a function of gap size.

Table 1
The Bird-Carreau model parameters determined from log-log plots of η vs $\dot{\gamma}$ and η^* vs ω.

Bird-Carreau model parameters	
λ_1	1.81
α_1	5
λ_2	200
α_2	5.1
η_o	1177.96
$(1-\alpha_1)/\alpha_1$	−0.80
$(1-\alpha_1)/\alpha_2$	−0.82
$(1+\alpha_1-\alpha_2)/\alpha_2$	0.18

The average of three measurements for each gap size were reported. The average of stress waves as a function of gap size superimposed nicely and no evidence of lip was observed. (Yoshimura and Prud'homme, 1988). Clearly the combination of cross-hatched texture of the upper plate and the No.100 medium textured sandpaper on the lower plate encroached on the sample strongly enough like Velcro to prevent any significant slip that would cloud the impact of non-linear viscoelasticity.

2.3. Data analysis

The nonlinear rheological behavior of tomato paste was determined by observing strain dependence at different frequencies in the transition mode of the strain sweep measurement. The first step of data analysis is transformation of data from time domain to frequency domain by Fourier transformation. The extraction of harmonics, recasting of both harmonics and sinusoidal waves and determination of LAOS parameters were done by using the

Table 2
Linear regression results for predicted rheological property versus the experimental measurements.

Function	Slope	Intercept	Correlation coefficient
η	−0.80	2.59	0.999
η^*	−0.80	3.35	0.997
ψ_1	−2.53	2.3	0.999
η'	−0.822	3.24	0.997
η''/ω	−0.85	2.61	0.998

Table 3
The dependence of strain at the crossover of G' and G'' on frequency of tomato paste.

Frequency (rad/s)	The strain at crossover of G' and G'' (%) (Pa)	The onset strain of the transition from linearity to non-linearity (%)
0.5	26.0 ± 1.3	0.21 ± 0.003
1	24.7 ± 1.8	0.12 ± 0.0003
5	23.6 ± 1.1	0.07 ± 0.00007
10	23.5 ± 2.1	0.07 ± 0.00001
15	23.5 ± 2.8	0.07 ± 0.00006

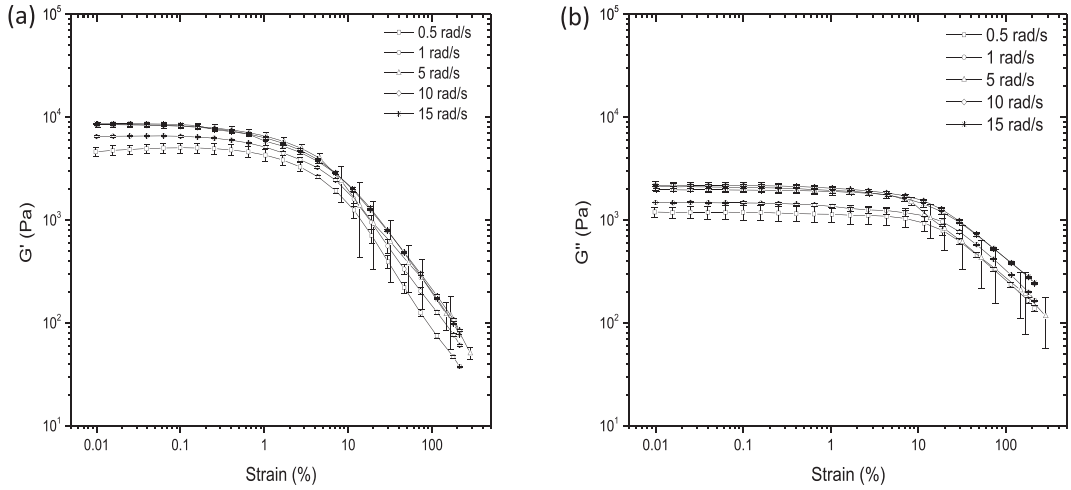

Fig. 3. Strain sweep plots of tomato paste at frequencies of 0.5, 1, 5, 10 and 15 rad/s, respectively. (a) G' vs γ and (b) G'' vs $\dot{\gamma}$.

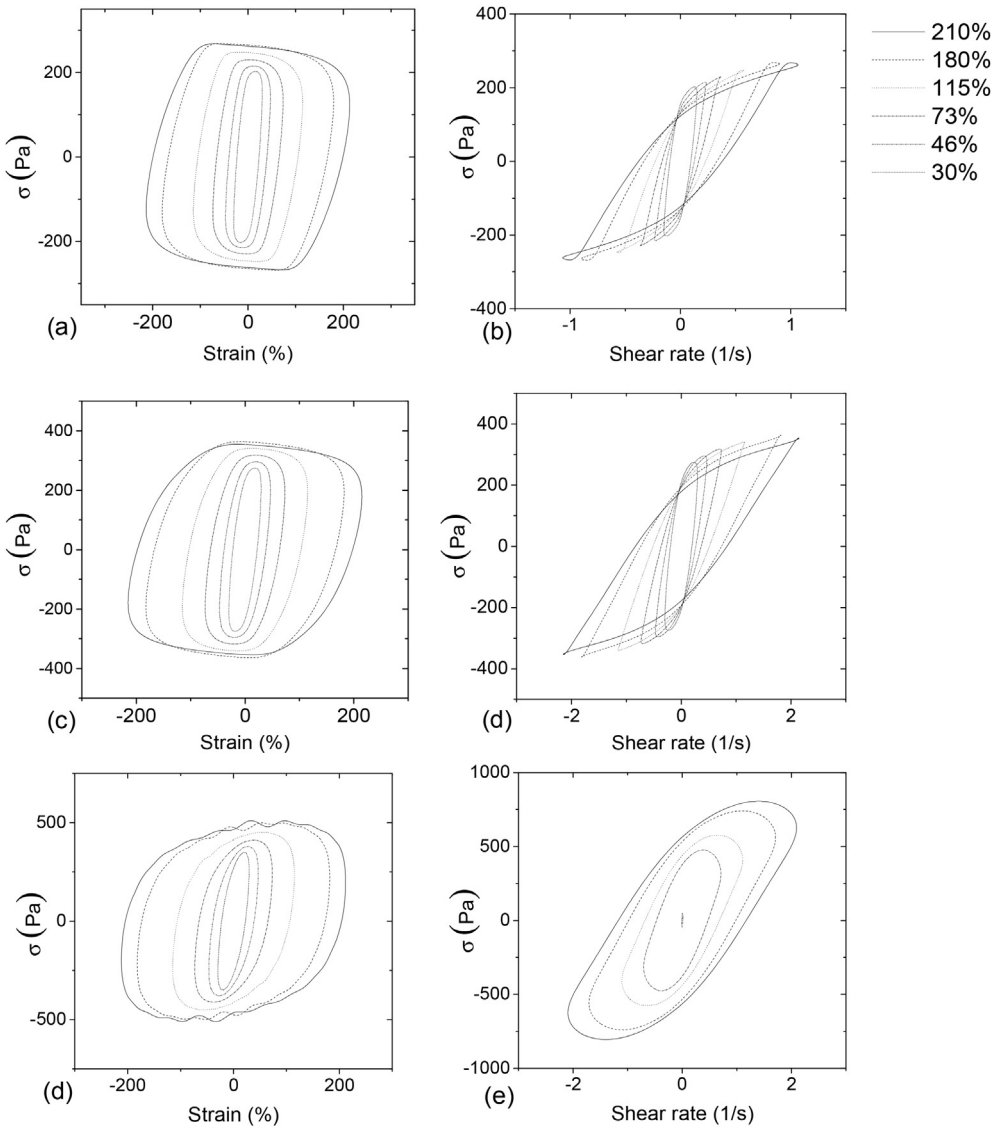

Fig. 4. The un-normalized LB loops of tomato paste in elastic and viscous perspectives at strains of 30, 46, 73, 115, 180, 210% at different frequencies: (a,b) 0.5, (c,d) 1, (e,f) 15 rad/s.

software of TA instruments. MATLAB algorithm was used to solve the differential equations of single-mode Giesekus Model to predict the intracycle stress response of tomato paste. ODE 45 differential equation solver was used with absolute and relative tolerances of 10^{-10}. Two different approaches were used in the simulation of SAOS and LAOS behavior of tomato paste. The model parameters of a single-mode Giesekus model were varied, however, the initial values of the model parameters were taken as $(\lambda = 42\ s,\ (\eta_o = \eta_T + \eta_s) = 466.01,$ and $\alpha = 0.4)$ from the stress relaxation and small amplitude oscillatory data, where T and S stand for tomato paste solvent. The tomato paste and water viscosities were as taken as 466 and 0.01 Pa s, respectively. These rheological parameters and frequency (0.5, 1, 5, 10 and 15 rad/s) values were entered in the Matlab code to simulate the stress response at each strain studied (0.01, 46, 115, 180 and 210%). The model parameters were varied and the experimental data was predicted.

3. Results and discussion

3.1. Prediction of the SAOS behavior of tomato paste by using Bird-Carreau model

The steady shear viscosity η, the complex viscosity η^*, the in phase η' and out of phase η'' components of the complex viscosity as well as the primary normal stress coefficient ψ_1 are all shown in Fig. 2 as a function of strain rate and frequency at a strain of 0.5% where tomato paste is linear viscoelastic. Tomato paste is non-linear above 0.25% strain level. Nonlinearity in tomato paste is the result of decay in the particle network whose relaxation time is much larger compared to the available experiment time during an oscillation for recovery and is unable to recover. Tomato paste shows Newtonian behavior at very low share rates below 0.01 sec^{-1}, becomes non-Newtonian beyond the shear rate of 0.1 sec^{-1} and does not appear to show other observable structural transitions. No zero shear viscosity trend was observed in SAOS data; complex viscosity and it's in phase and out phase components all showed power-law behavior. The model parameters of the Bird-Carreau model were obtained from the steady viscosity and complex viscosity and the model was validated using the primary normal stress coefficient data. These are shown in Table 1. The experimental data are all well simulated by the Bird-Carreau model. Comparison of experimental data versus the predicted data shows a high degree of superposition throughout the range of steady shear and dynamic viscosities. Regression analysis results for all rheological properties are shown in Table 2.

The prediction of the primary normal stress coefficient shown in Fig. 2c is very good considering that the parameters to predict the primary normal stress coefficient came from steady shear and dynamic viscosity data as the model necessitates. This validates the appropriateness of the Bird-Carreau model to describe the rheology of tomato paste and makes the model a predictive model rather than a curve fitting of the date by the equations. In the range of shear rates and frequencies tested there is a very high degree of superposition of the experimental data and predicted primary normal stress coefficient. The ability to accurately predict the SAOS behavior of tomato paste with a fundamental semi empirical constitutive model has never been done before. The Bird-Carreau

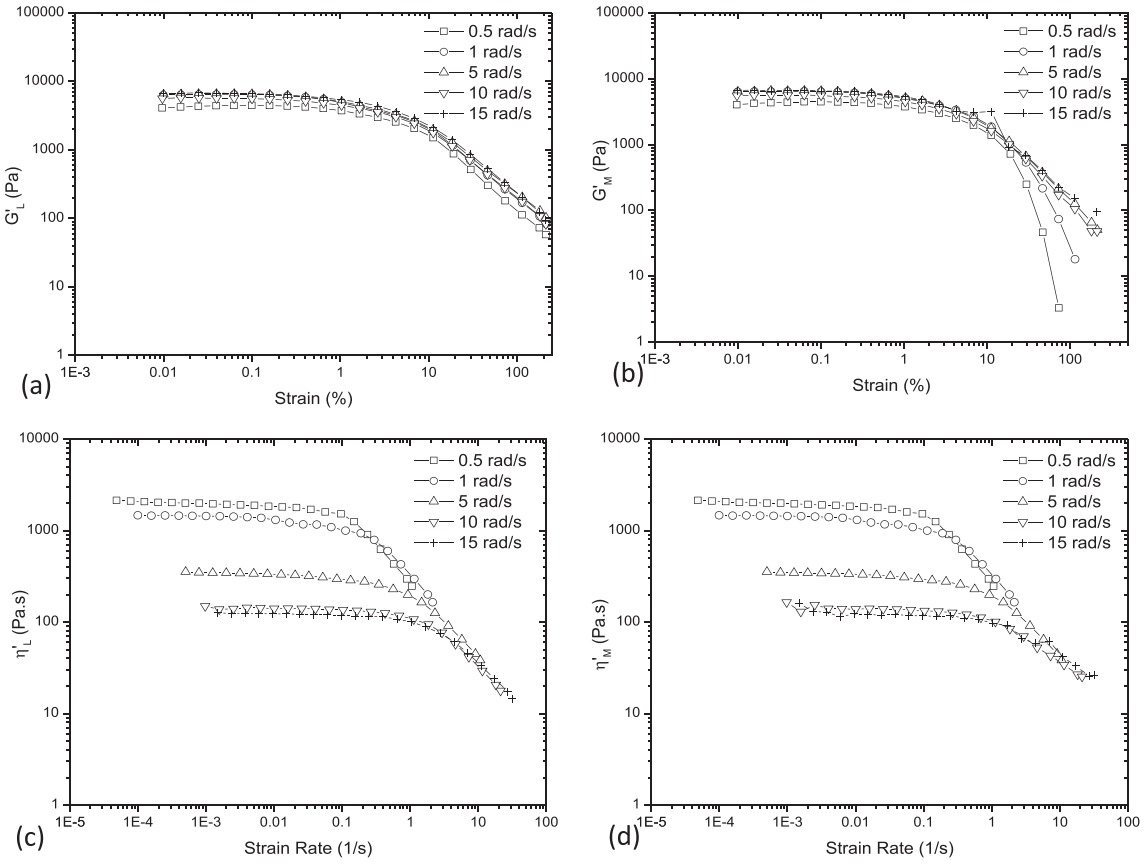

Fig. 5. The variation of (a) G'_M, (b) G'_L, (c) η'_M, and (d) η'_L with respect to γ of tomato paste.

model, although semi-empirical, provides the accuracy and the versatility which should make it of particular interest to those working with various food suspensions.

3.2. LAOS behavior of tomato paste

Strain thinning was observed in strain sweeps regardless of frequency for tomato paste where the onset of non-linear behavior is at about 0.1% of strain. Both the storage (G') and loss (G'') moduli showed a sharp decrease in the non-linear region indicating strong shear-induced structural changes within the fluid. In the linear region, G' was much larger than G'' which is consistent with a network structure made of solid constituents of tomato paste suspended in a pectin serum (Dervisoglu and Kokini, 1986; Chou and Kokini, 1987). Both G' and G'' of tomato paste stayed constant in the linear region by increasing frequency up to 15 rad/sec (Fig. 3). The resistance to the destruction of a network structure which is composed of interconnected aggregates of soft tomato particles resulted in increasing G' with increasing frequency. The stress response and elastic and viscous components became higher especially at higher frequencies because of the incomplete microstructural arrangement in the time span for each reversal movement of oscillatory shear. The nonlinearity began at 0.1% of strain and the crossover of G' and G'' was at 24.7% of strain at 1 rad/s (see Table 3). The transition from linear viscoelastic to nonlinear viscoelastic behavior and the crossover of G' and G'' were observed at lower strains as frequency was increased (Table 3) due to larger energy delivery to the system in a shorter timescale which had an impact on the extent of strain-induced structure decay.

The un-normalized LB loops may help to visualize how stress response evolves with strain/strain rate (Fig. 4). The stress loops versus strain and strain rate become bigger and their direction and shape change significantly as the strain increases because the delivered energy progressively increases. The stored and dissipated energy are related to the area on the stress-strain and stress-strain rate plots, respectively (Lauger and Stettin, 2010). These areas are growing as the strain increases. In the elastic analysis of the stress response (Fig. 4a, c, d) strain stiffening was observed indicated by the upward turn of shear stress at large strains. In the viscous analysis, a self-intersection was clearly observed at a frequency of 0.5 rad/s (Fig. 4b) resulting in a loop. This behavior disappeared at higher frequencies (>1 rad/s) (Fig. 4d and e). Secondary loops have been observed for many different fluids such as molten polymers (Stadler et al., 2008), polystyrene solutions (Hoyle et al., 2014), xanthan gum solutions (Carmona et al., 2014), foams (Ptaszek, 2015) and polymer-clay suspensions (Hyun et al., 2012) in the stress-strain rate plane. Mathematical predictions have been offered by Ewoldt et al. (2008) and our data once more confirms his predictions. The counter clockwise rotation of the loops in the viscous analysis is the indication of gradual softening which is interpreted as shear thinning behavior in non-linear region.

The variation of G'_M and G'_L with respect to strain is given in Fig. 5. $G'_M = G'_L = G'_1$ in the linear region and G' started to decrease beyond the critical strain of 0.25%. The G'_M and G'_L increased from

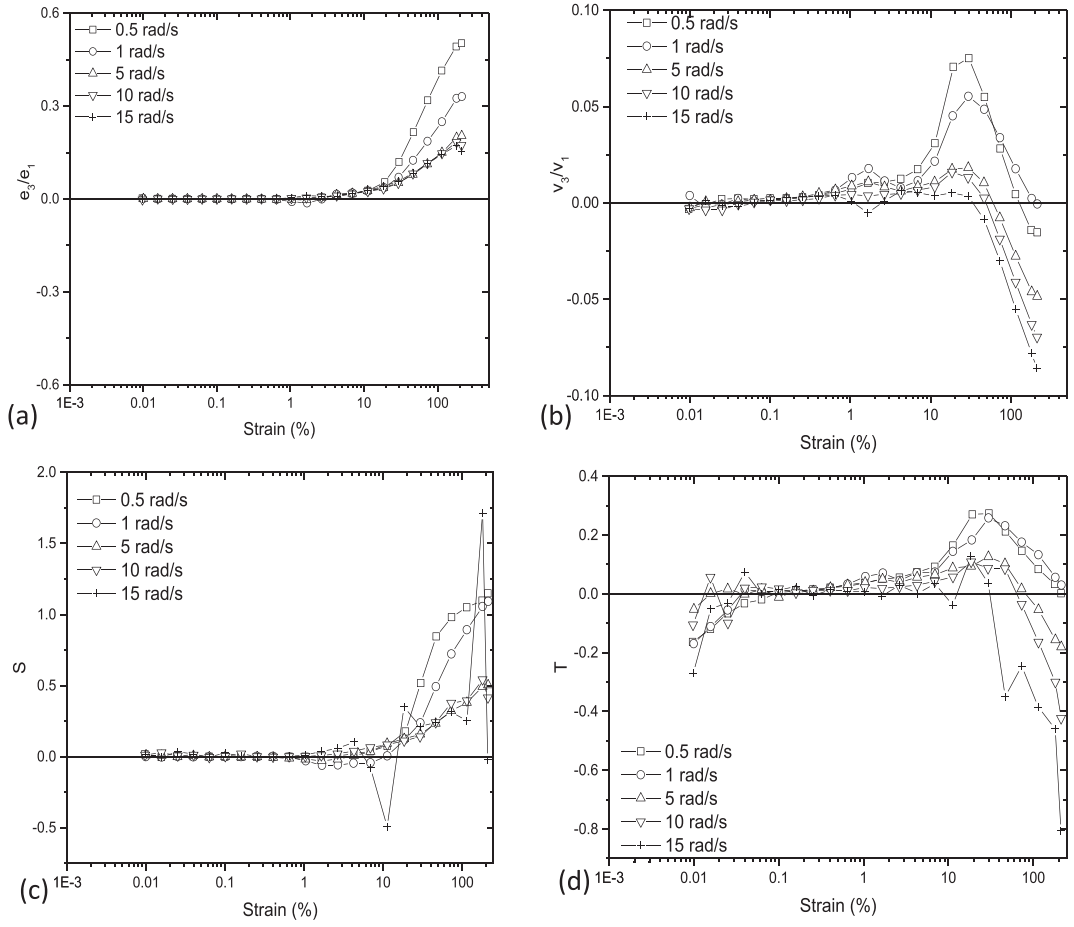

Fig. 6. The variation of (a) e_3/e_1, (b) v_3/v_1, (c) S and (d) T vs $\gamma(\%)$ of at different frequencies.

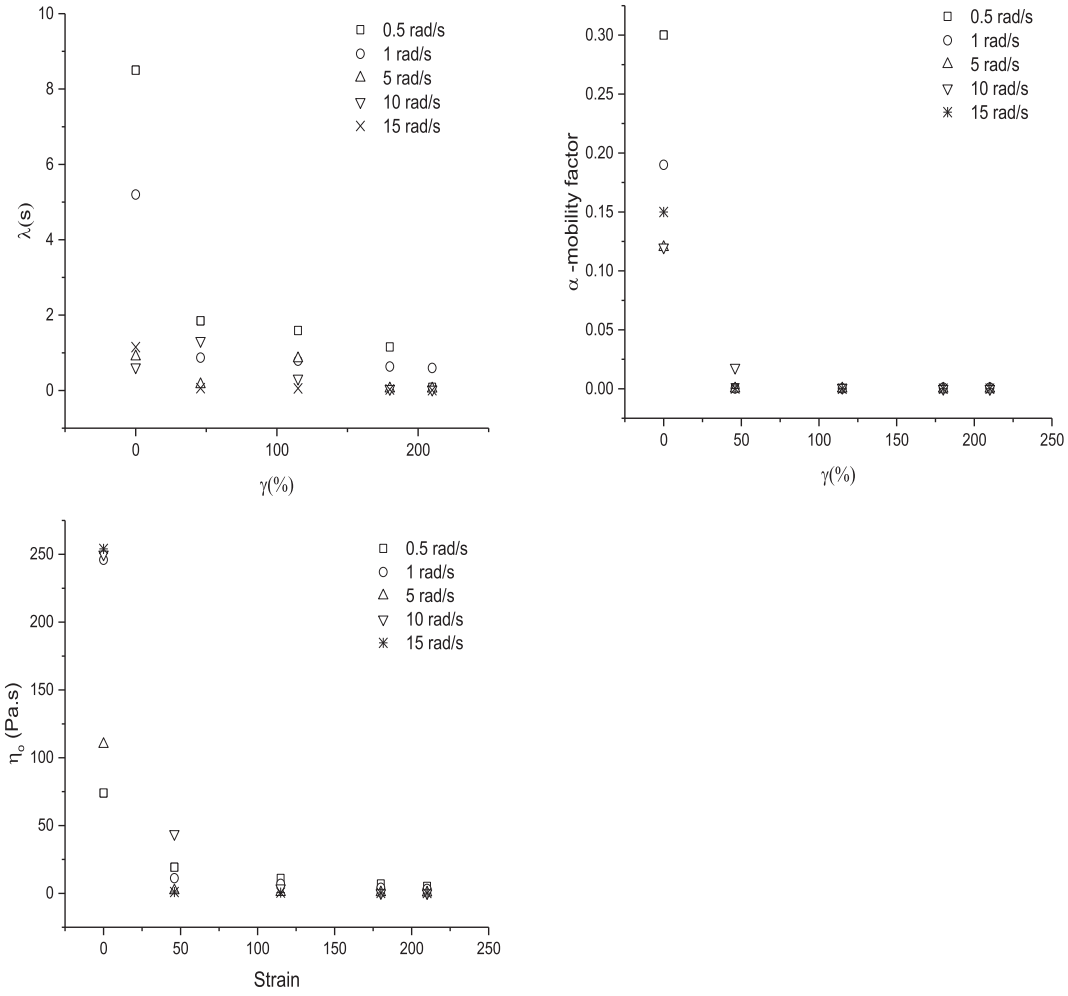

Fig. 7. The dependence of single mode Giesekus model parameters, (a) relaxation time (λ), (b) mobility factor (α) and (c) zero-shear viscosity (η_o), on strain and frequency.

4355 to 6325 Pa and from 4352 to 6315 Pa, respectively as the frequency increased from 0.5 to 15 rad/s at a strain of 0.25%. G'_M became more frequency dependent in the non-linear region when a linear curve fitting was done in a strain range of 1–200% (slope of −16.04 and −19.72 at 0.5 rad/s and 15 rad/s, respectively). G'_M became smaller as tomato paste was subjected to large strains and change in the direction of normalized LB loops. This behavior might indicate that tomato paste partially held its microstructure beyond the linear region due to the presence of pectin serum (Chou and Kokini, 1987) where the adhesiveness and flexibility of the pectin molecules facilitated the interconnection of tomato particles and also facilitated the progressive orientation within the structure by offering a lubrication phenomenon.

The large amplitude minimum rate viscosity η'_M and large rate viscosity η'_L showed a decreasing trend with strain rate which corresponded to shear thinning behavior (Fig. 5c and d). The maximum strain rate in LAOS was 2.07, 2.47 and 32 1/s when frequency was 0.5, 1, and 15 rad/s, respectively.

The elastic and viscous indicators of nonlinearity (e_3/e_1, v_3/v_1, S and T) plotted in Fig. 6 were all dependent on both strain and frequency. The non-linear viscoelastic behavior at higher frequencies was different than the behavior at lower frequencies due to the lack of time for the structure to be rebuilt. Strain hardening ($e_3/e_1 > 0$) which was never reported before for tomato paste was observed after a strain of 2.65%; also tomato paste shows shear thickening behavior never reported before depending on the frequency applied. An increase in frequency significantly changed the v_3/v_1 after 0.65% strain. There was a strong frequency dependence in the strain range of 0.65–4.32% which is considered as the mid-nonlinear region (MAOS) where we observe a local maximum or minimum depending on frequency. Tomato paste shows a shear thickening or shear thinning behavior depending on the magnitude of train and frequency as shown in Fig. 6b. The intracycle shear thickening behavior, again never reported before showed a maximum (~30 and ~18% of strain for a frequency of 0.5 rad/s and 15 rad/s, respectively) followed by a decreasing trend. Similarly but somewhat less pronounced results are observed when the S and T ratios were considered.

3.3. Prediction of non-linear LAOS behavior of tomato paste by using the single-mode Giesekus model

The nonlinear oscillatory shear flow of tomato paste was approximated by a single-mode Giesekus model. It contains quadratic nonlinearity and the stress tensor is divided into two parts: stress related with the solvent contribution (σ_S) and the polymer contribution (σ_P).

$$\sigma = \sigma_P + \sigma_S$$

The single mode Giesekus model (with three model parameters: λ, $\eta_0(=\eta_p+\eta_s)$ and α) and experimental data were compared by

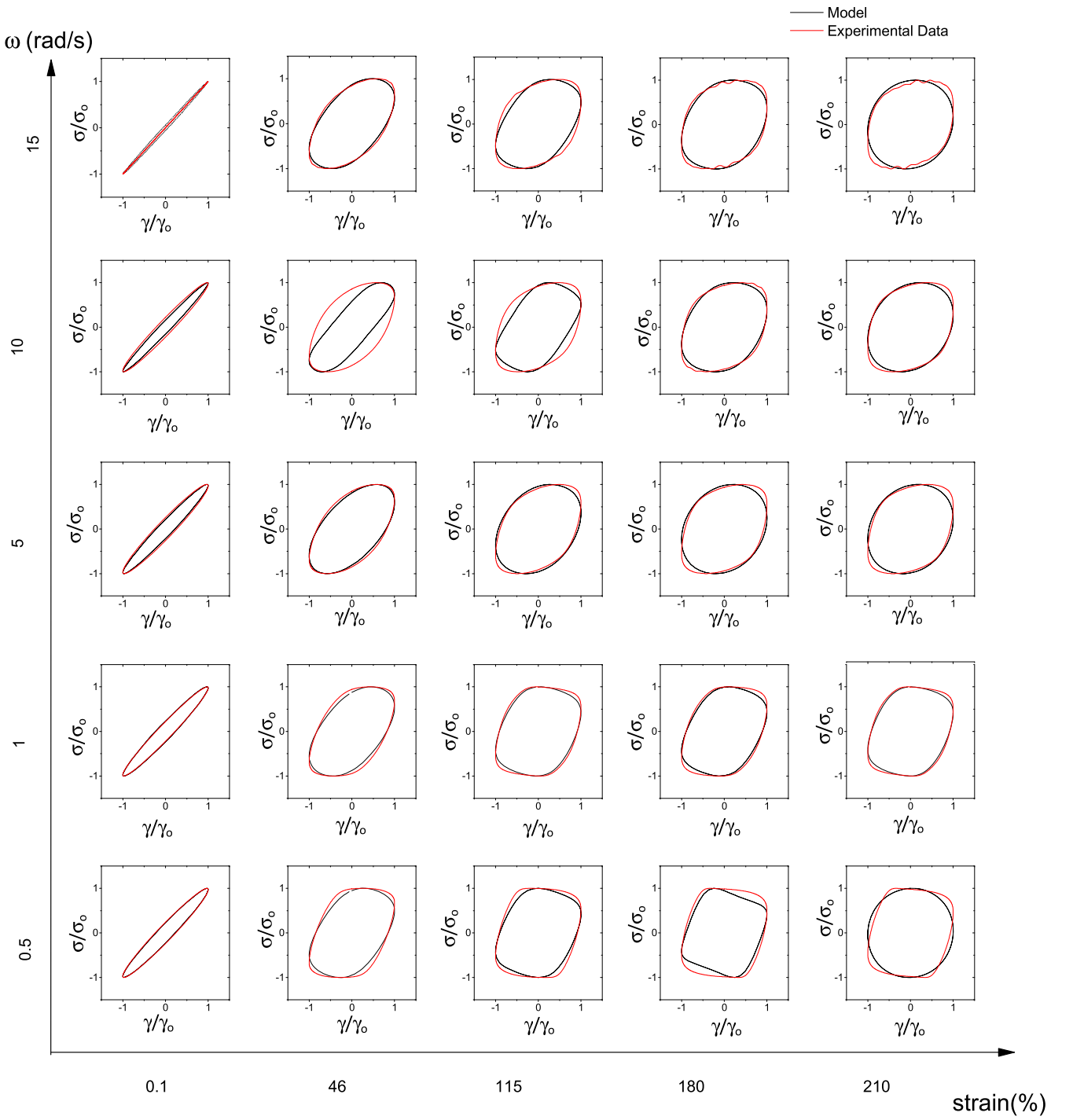

Fig. 8. The normalized elastic response of LB loops of tomato paste at different strains (0.01, 47, 115, 180 and 210% of strain) and frequencies (0.5, 1, 5 10 and 15 rad/s). Elastic LB loops are plotted "$\sigma(t)/\sigma_{max}$ and $\sigma'(t)/\sigma'_{max}$" vs $\gamma(t)/\gamma_0$ The black solid lines and dashed red lines are indicated Single-Mode Giesekus model and experimental data, respectively. (For interpretation of the references to colour in this figure legend, the reader is referred to the web version of this article.)

plotting the normalized stress response with respect strain and strain rate. The formation of secondary loops observed for the experimental data were successfully predicted by the Giesekus model (the model with following model parameters: λ, η_0 ($=\eta_p+\eta_s$) and α) consistent with earlier attempts (Ewoldt et al., 2008; Ewoldt and McKinley, 2010; Rogers and Lettinga, 2011). It appears that the non-linear dependence of tomato paste on strain and frequency for both elastic and viscous response cannot be predicted by using a fixed relaxation time and viscosity necessitated by the Giesekus model. In fact, two studies (Ewoldt et al., 2008; Rogers and Lettinga, 2011) used variable frequencies and a relaxation time ($\lambda = 1$ s) to give Deborah numbers ($De = \lambda\omega$) that are in the range of 0.01 to 10^3 in order to obtain successful predictions of SAOS and LAOS behavior of gluten dough for multi-mode Giesekus model. In their study, the model contains two relaxation times (λ_1 and λ_2). The model parameters were $\lambda_1 = 1$ s, $\eta_s = 0.01$ Pa s, $\eta_o = 10$ Pa s, $\lambda_2 = \lambda_1(\eta_s/\eta_p) = 0.001$ and $\alpha = 0.3$ for gluten dough. These model parameters simulated the experimental

data of gluten dough well. However, when fixed model parameters ($\lambda = 42\ s,\ \left(\eta_o = \eta_p + \eta_s\right) = 466,$ and $\alpha = 0.4$) for tomato paste was used, the LAOS behavior was poorly predicted. This might be related to having more liquid like rheological behavior rather than elastic behavior due to the progressive increase in strain which changes the structure as it dismantles. Hence, the model parameters were varied (λ, $\eta_0 = \eta_p + \eta_s$ and α) and were changed to fit the experimental data. These parameters are reported as a function of strain and frequency in Fig. 7. All parameters showed a decreasing trend as the strain increased regardless of frequency. This shows that the progressive increase in strain changes the structure of tomato paste and also the flow properties like relaxation time and viscosity. When the single mode Giesekus model used the parameters obtained as a function of strain and frequency predicted linear and non-linear behavior of tomato paste very well (Figs. 8 and 9).

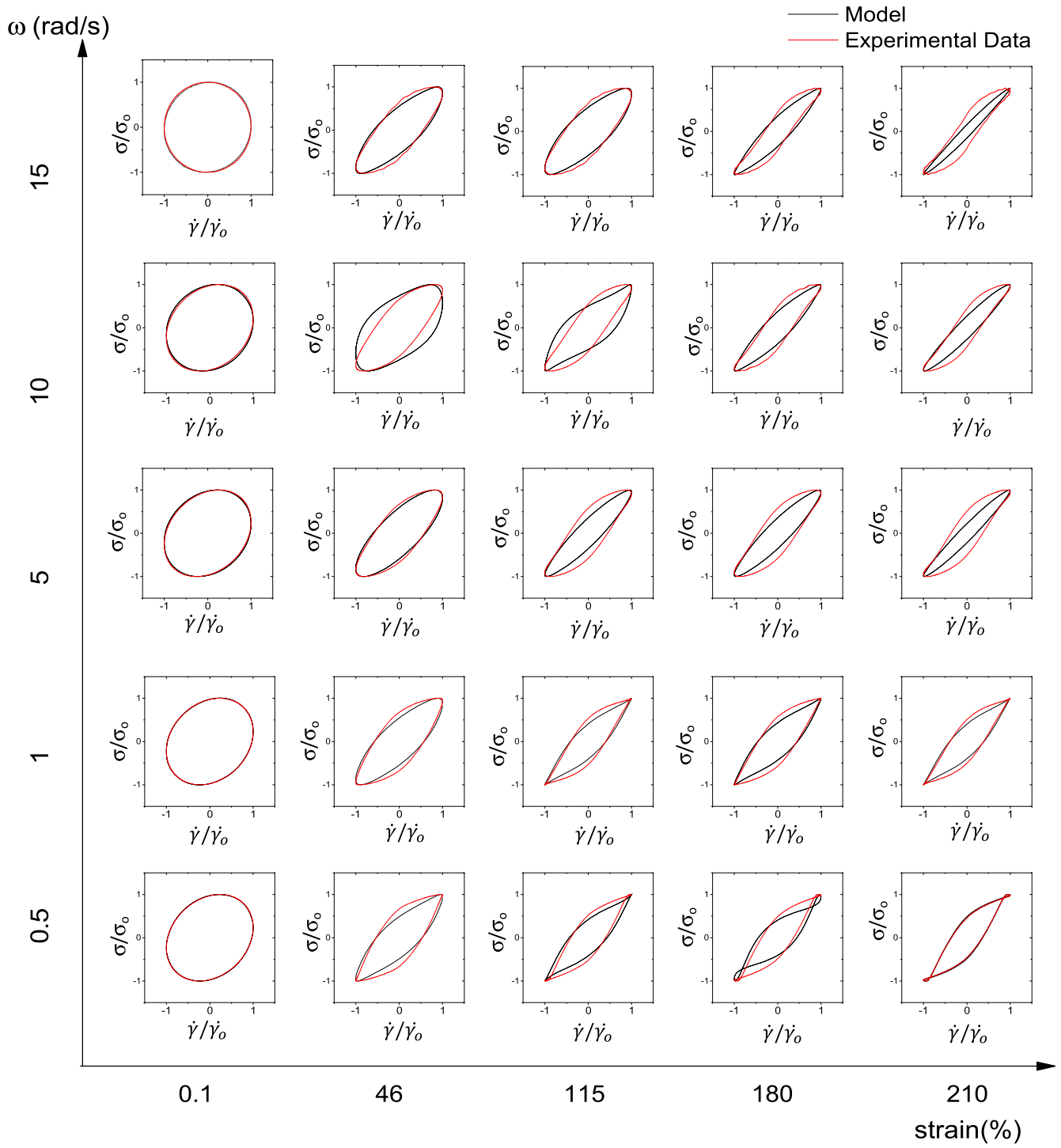

Fig. 9. The normalized viscous response of LB loops of tomato paste at different strains (0.01, 47, 115, 180 and 210% of strain) and frequencies (0.5, 1, 5 10 and 15 rad/s). Viscous LB loops are plotted "$\sigma(t)/\sigma_{max}$ and $\sigma''(t)/\sigma''_{max}$" vs $\dot{\gamma}(t)/\dot{\gamma}_0$. The black solid lines and dashed red lines are indicated single-mode Giesekus model and experimental data, respectively. (For interpretation of the references to colour in this figure legend, the reader is referred to the web version of this article.)

Each model parameter plays an important role on the prediction of experimental data and the fit of the LB loops, especially in the non-linear region. The relaxation time (λ) controls the width of the LB loops: as λ increases the elastic response becomes narrower and the viscous response becomes wider and the secondary loops disappear. The model parameter, α, controls the shape and extent of secondary loops in the viscous response. As α increases the secondary loops form in the viscous response. The total viscosity, η_o, controls the intensity of stress response. As η_o becomes higher, the stress response becomes higher. The Single mode Giesekus model fitted the experimental data well, however, the viscous response of LB loops at the highest frequency (15 rad/s) and the highest strain (200% of strain) needed the variable parameter approach.

4. Conclusions

The nonlinear SAOS viscoelastic behavior of tomato paste was very well predicted by the semi-empirical Bird-Carreau non-linear constitutive model. With the advent of the new and elegant Ewoldt-McKinley theory (Ewoldt et al., 2008), new rigorous non-linear rheological parameters (G'_M, G'_L, η'_M, η'_L, e_3/e_1, v_3/v_1, S and T) are utilized in this study to develop deeper insights related to the non-linear behavior of tomato paste. The sharp decrease in the G' and G'' with applied strain showed the nonlinearity. The emergence of non-linearities in LAOS was observed by the change in elliptical shaped curves in elastic and viscous and the non-linearity of elastic and viscous components of stress in LB loops at different frequencies. The counter-clockwise rotation of the loops is the indication of gradual softening. Strain stiffening was observed by the upward turn of shear stress at large strains. Increasing strain resulted in bigger loops of stress response and a change in the shape and orbital direction. Clockwise rotation of inner loops (at low strains) corresponded to strain softening which was followed by strain stiffening observed by upward turn of stress response in LAOS. Irreversible microstructural changes in the concentrated tomato paste dispersion are expected during flow reversal from the preceding cycle and subsequent increasingly poor reorganization of the structure as the strain and frequency increased. Single mode Giesekus model for the prediction of LB loops in SAOS and LAOS was used and the use of constant model parameters in model led to good predictions up to moderate strains and frequencies but poor predictions at high frequencies and strains. The use of varied model parameters in single mode Giesekus model showed very good fit to the experimental data. At high strains and frequencies, a variable parameter model was necessary to obtain a good fit of the LB loops.

References

Agusto, P.E.D., Falguera, V., Cristianini, M., Ibarz, A., 2012. Rheological behavior of tomato juice: steady-state shear and time-dependent modeling. Food Bioprocess Technol. 5, 1715–1723.

Atalik, K., Keunings, R., 2002. Non-linear temporal stability analysis of viscoelastic plane channel flows using a fully-spectral method. J. Newt. Fluids 102, 299–319.

Bae, J.-E., Lee, M., Cho, K.S., Seo, K.H., Kang, D.-G., 2013. Comparison of stress-controlled and strain-controlled rheometers for large amplitude oscillatory shear. Rheol. Acta 52, 841–857.

Bayod, E., Tornberg, E., 2011. Microstructure of highly concentrated tomato suspensions on homogenization and subsequent shearing. Food Res. Int. 44, 755–764.

Bayod, E., Mansson, P., Innings, F., Bergenstahl, B., Tornberg, E., 2007. Low shear rheology of concentrated tomato products. Effect of particle size and time. Food Biophys. 2, 146–157.

Bayod, E., Willers, E.P., Tornberg, E., 2008. Rheological and structural characterization of tomato paste and its influence on the quality of ketchup. Food Sci. Technol. 41, 1289–1300.

Bistany, K.L., Kokini, J.L., 1983a. Comparison of steady shear rheological properties and small amplitude dynamic viscoelastic properties of fluid food materials. J. Texture Stud. 14, 113–124.

Bistany, K.L., Kokini, J.L., 1983b. Dynamic viscoelastic properties of foods in texture control. J. Rheol 27, 605–620.

Carmona, J.A., Ramirez, P., Calero, N., Munoz, J., 2014. Large amplitude oscillatory shear of xanthan gum solutions. Effect of sodium chloride (NaCl) concentration. J. Food Eng. 126, 165–172.

Cho, K.S., Hyun, K., Ahn, K.H., Lee, S.J., 2005. A geometrical interpretation of large amplitude oscillatory shear response. J. Rheol. 49, 747–758.

Chou, T.D., Kokini, J.L., 1987. Rheological properties and conformation of tomato paste pectins, citrus and apple pectins. J. Food Sci. 52, 1658–1664.

Connelly, R.K., Kokini, J.L., 2003. 2D numerical simulation of differential viscoelastic fluids in a single-screw continuous mixer: application of viscoelastic finite element methods. Adv. Polym. Technol. 22 (1), 22–41.

Dervisoglu, M., Kokini, J.L., 1986. Steady shear rheology and fluid mechanics of four semi-solid foods. J. Food Sci. 51, 541–546.

Dervisoglu, M., Kokini, J.L., 1990. Wall effects in the laminar pipe flow of four semi-solid foods. J. Food Eng. 11, 29–42.

Dhanasekharan, M., Huang, H., Kokini, J.L., 1999. Comparison of observed rheological properties of hard wheat flour dough with predictions of the Giesekus-Leonov, White-Metzner and Phan-Thien Tanner models. J. Texture Stud. 30, 603–623.

Dhanasekharan, M., Wang, C.F., Kokini, J.L., 2001. Use of nonlinear differential viscoelastic models to predict the rheological properties of gluten dough. J. Food Process Eng. 24, 193–216.

Dogan, H., Kokini, J.L., 2007. Rheological Properties of Foods, Handbook of Food Engineering 2nd Edition 2-115. CRC Press.

Dus, S.J., Kokini, J.L., 1990. Prediction of the nonlinear viscoelastic properties of a hard dough wheat flour dough using the Bird-Carreau constitutive model. J. Rheol. 34, 1069–1084.

Duvarci, O.C., Yazar, G., Kokini, J.L., 2017. The comparison of LAOS behavior of structured food materials (suspensions, emulsions and elastic networks). Trends Food Sci. & Technol. 60, 2–11.

Ewoldt, R., McKinley, G.H., 2010. On secondary loops in LAOS via self-intersection of Lissajous–Bowditch curves. Rheol. Acta 49, 213–219.

Ewoldt, R.H., Hosoi, E., McKinley, G.H., 2008. New measures for characterizing nonlinear viscoelasticity in large amplitude oscillatory shear. J. Rheol. 52, 1427–1458.

Foungfuchat, A., Seetapan, N., Makmoon, T., Pongjaruwat, W., Methacanon, P., Gamonpilas, C., 2012. Linear and non-linear viscoelastic behaviors of cross-linked tapioca starch/polysaccharide systems. J. Food Eng. 109, 571–578.

Giesekus, H., 1982. A simple constitutive equation for polymer fluids based on the concept of deformation-dependent tensorial mobility. J. Newt. Fluid Mech. 11, 69–109.

Graham, M., 1995. Wall slip and the nonlinear dynamics of large amplitude oscillatory shear flows. J. Rheol. 39, 697–712.

Gunasekaran, S., Ak, M.M., 2002. Cheese Rheology and Texture. CRC Press.

Hoyle, D.M., Auhl, D., Harlen, O.G., Barroso, V.C., Wilhelm, M., McLeish, T.C.B., 2014. Large amplitude ascillatory shear and Fourier transform rheology analysis of branched polymer melts. J. Rheol. 58, 969–997.

Hyun, K., Wilhelm, M., Klein, C.O., Cho, K.S., Nam, J.G., Ahn, K.H., Leed, S.J., Ewoldt, R.H., McKinley, G.H., 2011. A review of nonlinear oscillatory shear tests: analysis and application of large amplitude oscillatory shear (LAOS). Prog. Polym. Sci. 36, 1697–1753.

Hyun, K., Lim, H.T., Ahn, K.H., 2012. Nonlinear response of polypropylene (PP)/Clay nanocomposites under dynamic oscillatory shear. Korea-Ausralia Rheol. J. 24, 113–120.

Joyner, H.S., Meldrum, A., 2016. Rheological study of different mashed potato preparations using large amplitude oscillatory shear and confocal microscopy. J. Food Eng. 169, 326–337.

Kallus, S., Willenbacher, N., Kirsch, S., Distler, D., Neidhofer, T., Wilhelm, M., Spiess, H.W., 2001. Characterization of polymer dispersions by fourier transform rheology. Rheol. Acta 40, 552–559.

Kokini, J.L., Chou, T.C., 1993. Comparison of the conformation of tomato pectins with apple and citrus pectins. J. Texture Stud. 24 (2), 117–137.

Koocheki, A., Ghandi, A., Razavi, M.A., Mortazavi, S.A., Vasiljevic, T., 2009. The rheological properties of ketchup as a function of different hydrocolloids and temperature. Int. J. Food Sci. Technol. 44, 596–602.

Lauger, J., Stettin, H., 2010. Differences between stress and strain control in the non-linear behavior of complex fluids. Rheol. Acta 49, 909–930.

Melito, H.S., Daubert, C.R., Foeeding, E.A., 2013a. Relating large amplitude oscillatory shear and food behavior: correlation of nonlinear viscoelastic, rheological, sensory and oral processing behavior of whey protein isolate/-carrageenan gels. J. Food Process Eng. 36, 521–534.

Melito, H.S., Daubert, C.R., Foeeding, E.A., 2013b. Relationships between nonlinear viscoelastic behavior and rheological, sensory and oral processing behavior of commercial cheese. J. Texture Stud. 44, 253–288.

Mills, P.L., Kokini, J.L., 1984. Comparison of steady shear and dynamic viscoelastic properties of Guar and Karaya Gums. J. Food Sci. 49, 1–4.

Morrison, F.A., 2001. Understanding Rheology. Oxford University.

Ng, T.S.K, McKinley, G.H., Ewoldt, R.H., 2011. Large amplitude oscillatory shear flow of gluten dough: a model power-law gel. J. Rheol. 55, 627–654.

Plutchok, G., Kokini, J.L., 1986. Predicting steady and oscillatory shear rheological properties of CMC/guar blends using Bird-Carreau constitutive model. J. Food Sci. 51, 1284–1288.

Ptaszek, P., 2015. A geometrical interpretation of large amplitude oscillatory shear (LAOS) in application to fresh food foams. J. Food Eng. 146, 53–61.

Rao, M.A., 2007. Rheology of Fluid and Semisolid Foods: Principles and Applications. Springer.

Rathod, M., Kokini, J.L., 2014. Non-newtonian fluid mixing in a twin-screw mixer geometry: three-dimensional mesh development, effect of fluid model and operating conditions: non-newtonian fluid mixing in a twin-screw mixer. J. Food Eng. 169, 214–227.
Reimers, M.J., Dealy, J.M., 1998. Sliding plate rheometer studies of concentrated polystyrene solutions: nonlinear viscoelasticity and wall slip of two high molecular weight polymers in tricresyl phosphate. J. Rheol. 42, 527–548.
Rogers, S.A., Lettinga, M.P., 2011. A sequence of physical processes determined and quantified in large-amplitude oscillatory shear (LAOS): application to theoretical nonlinear models. J. Rheol. 56, 1–25.
Sahin, H., Ozdemir, F., 2004. Effect of some hydrocolloids on the rheological properties of different formulated ketchups. Food Hydrocoll. 18, 1015–1022.
Sanchez, M.C., Valencia, C., Gallepos, C., Ciruelos, A., Latorre, A., 2002. Influence of processing on the rheological properties of tomato paste. J. Sci. Food Agric. 82, 990–997.
Sanchez, M.C., Valencia, C., Ciruelos, A., Latorre, A., Gallepos, C., 2003. Rheological properties of tomato paste: influence of the addition of tomato slurry. J. Food Sci. 68, 551–554.
Stadler, F.J., Leygue, A., Burhin, H., Baily, C., 2008. The potential of large amplitude oscillatory shear to gain an insight into the long-chain branching structure of polymers. Polym. Repr. 49, 121–122.
Szopinski, D., Gerrit, G.A., 2016. Viscoelastic properties of aqueous guar gum derivative solutions under large amplitude oscillatory shear (LAOS). Carbohydr. Polym. 153, 312–319.
Tanglertpaibul, T., Rao, M.A., 1987. Rheological properties of tomato concentrates as affected by particle size and methods of concentration. J. Food Sci. 52, 141–145.
van der Vaart, K., Depypere, F., De Graef, V., Schall, P., Fall, A., Bonn, D., Dewettinck, K., 2013. Dark chocolate's compositional effects revealed by oscillatory rheology. Eur. Food Res. Technol. 236, 931–942.
Valencia, C., Sanchez, M., Ciruelos, A., Latorre, A., Madiedo, J.M., Gallegos, C., 2003. Non-linear viscoelasticity modeling of tomato paste products. Food Res. Int. 36, 911–919.
Vercet, A., Sanchez, C., Burgos, J., Mantanes, L., Buesa, P.L., 2002. The effects of manothermosonication on tomato pectic enzymes and tomato paste rheological properties. J. Food Eng. 53, 273–278.
Vyakaranam, K., Kokini, J.L., 2010. Advances in 3D numerical simulation of viscous and viscoelastic mixing flows. In: Food Engineering Interfaces. Springer, New York.
Wang, C.F., Kokini, J.L., 1995. Prediction of the nonlinear viscoelastic properties of gluten doughs. J. Food Eng. 25, 297–309.
Wilhelm, M.H., 2002. Fourier-transform rheology. Macromol. Mater. Eng. 287, 83–105.
Wilhelm, M.H., Maring, D., Spiess, H.W., 1998. Fourier-transform rheology. Rheol. Acta 37, 399–405.
Xu, S.-Y., Showmaker, C.F., Luh, B.S., 1986. Effect of break temperature on rheological properties and microstructure of tomato juices and pastes. J. Food Sci. 51, 399–402.
Yazar, G., Caglar Duvarci, O., Tavman, S., Kokini, J.L., 2016. Effect of mixing on LAOS properties of hard wheat flour dough. J. Food Eng. 190, 195–204.
Yazar, G., Duvarci, O., Kokini, J.L., Tavman, S., 2017. Non-linear rheological behavior of gluten-free flour doughs and correlations of LAOS parameters with gluten-free bread properties. J. Cereal Sci. 28–36.
Yoshimura, A.S., Prud'homme, R.K., 1988. Wall slip effects on dynamic oscillatory measurements. J. Rheol. 32, 575–584.
Yosick, J.A., Giacomin, J.A., Stewart, W.E., Ding, F., 1998. Fluid inertia in large amplitude oscillatory shear. Rheol. Acta 37, 365–373.